Rev.Adv.Mater.Sci. 6 (2004) 12-20

# APPLICATION OF IMAGE PROCESSING TO THE CHARACTERISATION OF NANOSTRUCTURES*

**Manuel F. M. Costa**

Universidade do Minho, Departamento de Fisica, Campus de Gualtar, 4710-057 Braga, Portugal

*Received: June 19, 2003*

**Abstract.** The inspection and characterization of nanomaterials and structures should be performed extensively and whenever possible in a non-invasive way. In recent years, a major development of image acquisition and digitalization systems was achieved as well as in what concerns image analysis and processing methods and tools. Those techniques are now being frequently used in metrology and characterization laboratories including in the fields of nanomaterials and systems. On this communication we will review the most relevant image acquisition and processing systems and techniques exemplifying with results of the work being performed at the Microtopography Laboratory and in collaboration with the Functional Coatings Group of the University of Minho.

* Presented at International Conference Nanomaterials and Nanotechnologies (Crete, Greece, August 30-September 6, 2003)

## 1. INTRODUCTION

The generalization of low cost high computational power microcomputers as well as cameras, digital cameras, image digitizers and processing boards lead, along last decade, to a dramatic growth of Image Processing (IP) not only in what concerns the development of an enlarged set of IP methods and techniques, but also in the number of applications in the widest variety of fields [1-7]. Most phenomena and processes in the physical world can be represented by bi- or multidimensional functions that with this development in IP can be suitably analyzed, understood, and processed.

According to the even more conservative estimates, more than 75 percent of all information received by the man is visual. Furthermore, its processing efficiency is remarkably high.

In this context, an enlarged set of efficient hardware, software, and IP methods and tools is nowadays readily available for application in the widest variety of fields in Science and Technology. In what concerns non-invasive inspection and characterization of micro and nanostructures, this is definitely also true.

Typically image processing (IP) deals with images which are two-dimensional entities (such as digital images, scanned photos or graphs, X-ray films, microscope images, satellite pictures, ...) captured electronically using a scanner or camera system that digitizes the spatially continuous co-ordinates resulting in a regularly spaced matrix filled with values within a discreet range. A digital image is a mapping from the real three-dimensional world to a set of two-dimensional discrete points. Each of these spatially distinct points holds a number that denotes intensity, amplitude, grey level or color for it, and can be conveniently fed to a digital computer for processing. Here, processing essentially means algorithmic recognition or analysis, enhancement and manipulation of the digital image data. Every image processing technique or algorithm takes an input, an image or a sequence of images, and produces an output: a modified image or a set of parameters and functions describing the content of the input image [1-14].

Corresponding author: Manuel F. M. Costa, email: mfcosta@fisica.uminho.pt

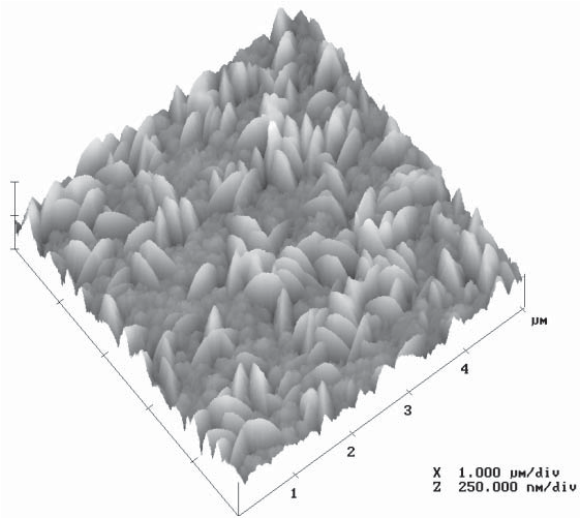


**Fig. 1.** AFM inspection of the surface of a 2.93 microns thick zirconium oxy-nitride film on an Inconel 738LC substrate. Tri-dimensional representation enhancing, by colour shading, the shape of the relevant surface structures.

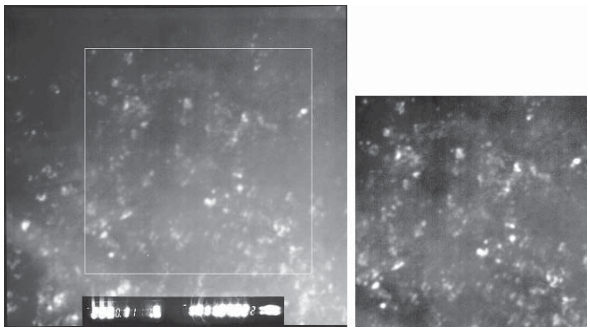

**Fig. 2.** The proper choice of a region of interest ROI is very important in any IP procedure. In the image on the right the illumination non-homogeneity was corrected in the ROI.

Although digital image processing is, by far, the most important one, analogue optical IP, including in real time, have also a major role. For instance, the implementation of Fourier processing techniques in the frequency domain gives excellent results, especially in the study of dynamic or transient processes. Furthermore, the concept of image as bidimensional entity can be easily generalized to 3D or even multidimensional image like structures processed with essentially the same tools as the conventional 2D images.

The interest of the application of IP in surface science seems obvious. Dependent on the scale, direct or indirect visual evaluation of the surface' structure is always sought. In micro and nanoscience and technology this is also true. A large number of characterization tools and methods produces as output two dimensional structures that can be seen as images and treated as such. In fact, Image Processing can be applied at smaller or larger extent to virtually all the range of available NDE techniques [14] including optical interferometer and profilometers or microtopographers of different kinds (ie. Nomarski and confocal microscopes, depth of focus, speckle, structured lightning, triangulation, ...), difractometers (Angle-Resolved Scattering, Total Integrated Scattering), elipsometers, spectroscopes and fluorescence spectrophotometers, photoacoustics and life-time spectroscopy systems, STM, AFM (Fig. 1), Raman spectroscopy, XRD, FTIR, Eddy currents, induced magnetic fields, thermal waves analysis, ultrasonic waves, X-ray, shearographers, holographic and tomographic systems, etc.

## 2. DEFINITIONS AND BASIC CONCEPTS

In the brief presentation that follows we shall consider the image, i.e. the object of our IP, as bidimensional functions as conventionally. Furthermore, we shall refer mostly to digital image processing in the Cartesian and Fourier spaces [1-13].

An image is considered to be a function of two real variables, for example, $I(x,y)$ of brightness (grey level, color component, ...) of the image at the real co-ordinate position $(x,y)$. In general, an image may be considered to be formed by or to contain subimages. All or some of those regions can be chosen as regions-of-interest (ROI) and processed, independently or not. This concept reflects the fact that images frequently contain collections of meaningful objects or structures. In modern sophisticated image processing system it should be possible to apply specific image processing operations to selected regions, while preserving the rest of it or else to preserve the selected ROI from its neighbor regions. The definition and unambiguous location of the ROI or ROIs in the image is the first task to be executed in an IP procedure. The proper choice of the ROI according to the image any *a priori* knowledge and our IP objectives is fundamental to the success of the processing sought (Fig. 2).

Image processing techniques are usually divided in two major categories: radiometric and geometri-

cal. In geometric operations in opposition to radiometric ones, the grey (color, or any other entity in general) level in each point (pixel) of the image is changed accordingly to the image' grey values on its neighborhood. Eventually the new grey level in one pixel can even be totally independent of its original value, for instance in edge detection (Fig. 5).

Radiometric operators act on the original images changing its brightness (color) distribution. In digital IP the image is represented by a 2D matrix that is processed typically by multiplication by another matrix or series of matrix sequentially.

## 3. BRIEF OVERVIEW OF FUNDAMENTAL IMAGE PROCESSING OPERATORS

There is a large number of well established IP operators available, from simple brightness reduction operators to complex neural network' skeletization and following operators. In virtually all IP procedures it is required the application of a series operators in a sequential clearly established way.

Bellow we provide a list of the most important operators or processing techniques. For some of the more useful ones in surface characterization, a brief description is provided together with a few examples of application [1-13]:

- Brightness and contrast
- Contrast stretching and histogram equalization and manipulation
- Binary operations
- Arithmetic-based operations
- Convolution-based operations in the spatial domain or in the frequency domain
- Smoothing operations
- Linear and non-linear filters
- Derivative-based operators
- Morphological operators - dilation and erosion, Boolean convolution, opening and closing, skeletonization, propagation
- Morphological smoothing, enhancing, and edge detection
- Shadowing correction
- Defocus correction
- Enhancement and restoration techniques
- Unsharp masking, noise suppression, distortion suppression, segmentation
- Thresholding and binarization
- Color manipulation
- Pseudo coloring
- Edge detection
- Processing in the Fourier space, spatial filtering, correlation and convolution
- Measuring and characterization (see case study).

### 3.1. Selection of the Region of Interest

Often the available images include parts that have little or no interest at all that thus can, and should, be removed or ignored (Fig. 2.). As pointed up above, one of the first steps in the image's processing is thus to define the region of interest (ROI) to process. When we intend to apply geometric (kernel) image processing operators, the most convenient ROI' shape is square or rectangular. However, some other different forms may be the best choice [7], i.e., circles when processing interferograms or even the complex shape of the boundary of a cracked or detached part of a thin film.

### 3.2. Homogenisation of image's brightness

Sometimes the images to be processed are acquired in conditions of non-even illumination or they present an inhomogeneous brightness distribution superimposed on the image features. This may cause major difficulties in the location or characterization of some features in certain areas of the image. It may even preclude the successful application of even advanced IP procedures [6]. In the example presented in Fig. 2 without performing first the homogenization of the brightness distribution in the ROI, it was impossible to apply binarization and blob analysis for an accurate calculation of the crystallinity of the thin film (26%) [15].

### 3.3. Improvement of image's contrast

The control of image's brightness and improve its contrast is one of the most frequently performed tasks. Most cameras are now prepared to make this type of image adjusts automatically in the acquisition process.

Radiometric operators are used and frequently based on the analysis and manipulation of the image's histogram. The histogram or probability density function is estimated by counting the number of times each brightness or grey level occurs in the image. An image with good contrast and illumination will give an histogram with peak more or less evenly distribute by all the available range of grey levels (frequently $2^8 = 256$). The image can be radiometrically changed by adjusting the shape of its histogram in a determined way.

An improvement of image' quality can be obtained by equalizing the image's histogram [3]. His-

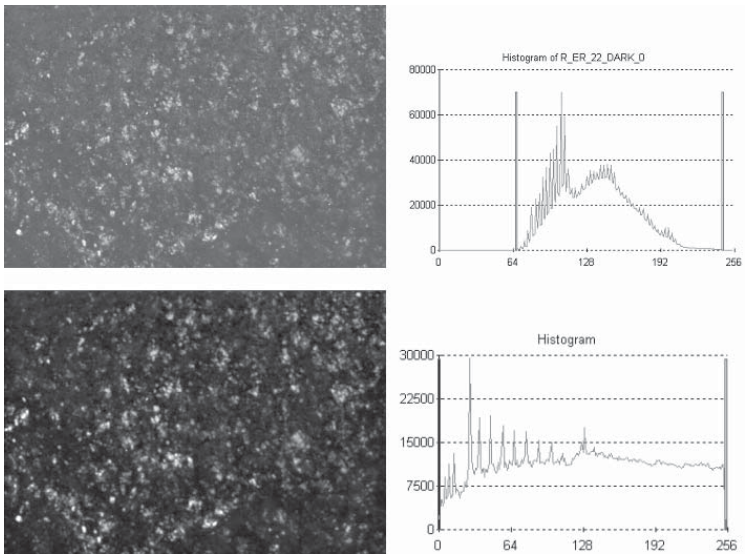


**Fig. 3.** Low contrast images (top left) can be improved by manipulation of its histogram (top right). A simple histogram stretching (bottom) gives a much clear image.

togram equalization operate by changing the grey level of the pixels in the image in a way that makes the final histogram to be uniform in all range of available grey levels. When we have a set of images acquired under different conditions, it is convenient to adjust them in order to be directly comparable. Histogram equalization is frequently used for this purpose. As in most IP procedures, it is however essential to select first the area of interest (ROI). The histogram equalization shall be performed only there, but not in the entire image. We first equalize basing on the ROI's histogram in the master channel. In color images, the histogram equalization can be performed also on each, all or just some, color channel.

In order to increase the image's contrast, it is often sufficient to 'stretch' its histogram. This is illustrated in Fig. 3. The height of each peak is maintained but dislocated in order to have a final image with pixels having brightness values in the full available range.

## 3.4. Noise reduction

Frequently the images to be processed are rather noisy (Fig. 4). Optical and electronic noise is added to the image during the process of image acquisition and digitalization. The high frequency noise that renders the image to have speckles depends on the degree and type of illumination, cameras' optical and electronic quality, and room temperature.

The use of microscopy in micro and nano science and technology is common to employ very high magnifications. The illumination is sometimes a problem and some amount of electronic amplification of the imaging system is often necessary, thus increasing the image's high frequency noise [10]. On the other hand, the reduced depth of field may result in defocusing in some areas of the acquired image. So the existence of images' blurring at some extent should be expected at least over some areas of the image. For these reasons, the smoothening of the image in order to reduce the high frequency noise should be done carefully. A simple image averaging on 2x2 or even 3x3 pixels may give acceptable results for the smoothening of the image. However, we suggest Fourier filtering, because it allows a tighter control of the images frequency content. In doing so, images blurring can be reduced to a minimum, while the high frequency noise will be removed. The bidimensional fast Fourier transformation (FFT) of the image is computed (see Section 3.7 below). The higher frequencies on the image that correspond mostly to undesirable noise can be removed from the image by applying a low pass filter. A smooth Gaussian or Butter-worth filter of second order with a carefully chosen frequency cut-off is a good choice preserving the faintest edges and removing the image noise. The inverse FFT is then applied to the new frequency spectrum obtained; this procedure results in the desired filtered smooth image.

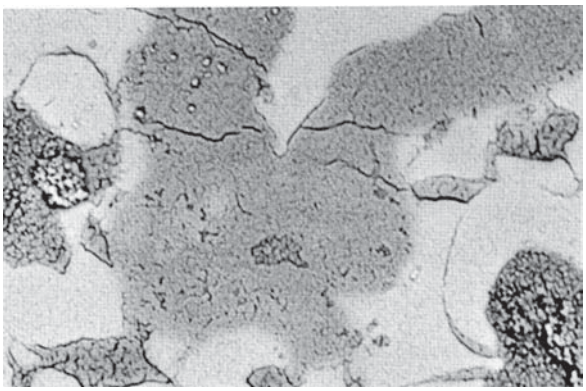

**Fig. 4.** 22x15 $\mu m^2$ SEM image obtained at 20 KeV. The SEM image shows microcracks in oxide grow of a thermal barrier coating (IN738LC substrate, interlayer VPS NiCoCrAlY, top layer APS: $ZrO_2$ - $8Y_2O_3$) after annealing at 1100 °C for 100 h in air.

## 3.5. Edge detection or enhancement

In order to turn more evident the location and limits of particular areas or structures like cracks or pits (Figs. 4 and 5), edge detection or enhancement procedures can be employed. A large variety of operators is available to be chosen accordingly to the image characteristics and requested processing outputs (morphological operators, linear geometrical operators, Sobel differential or Laplacian operators) [1-13]. Along with the application of the majority of these operators, any processing task will involve the application of a well established sequence of operations adjusted to the image to be dealt with and according to our processing requirements.

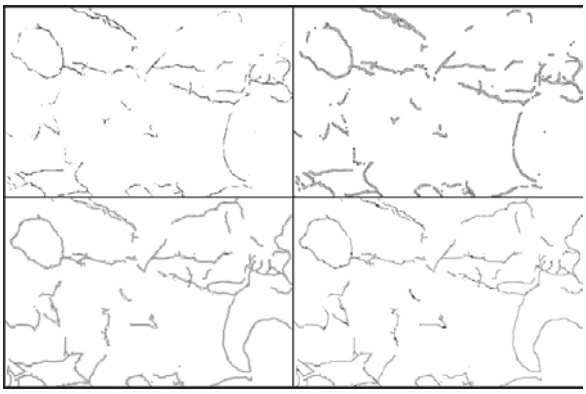

**Fig. 5.** Results of different edge detection procedures on the micrograph presented in Fig. 4. The successive application of radiometric and morphological operators allows a reasonable identification of the major relevant cracks on the structure (top left image). The application of a Sobel differential operator enhances its visibility (top right). Better results can be obtained by the application of a negative Laplacian edge detector (bottom left) or even an advanced following technique using neural network processing (bottom right).

## 3.6. Characterisation and measurement

A large number of characterization parameters are used in IP from the mean grey value, average or standard deviation, variance, mean peak spacing or correlation length to more complex function as autocorrelation [1,3,5,8], or normalized correlation function (Eq. (1)) an excellent tool to compare two images (for instance represented by functions $f(x,y)$ and $g(x,y)$.

$$\gamma_{fs}(x,y) = \frac{\int_{-\infty}^{+\infty} f(x',y')g^{*}(x'-x,y'-y)dx'dy'}{\int_{-\infty}^{+\infty} f(x',y')g^{*}(x',y')dx'dy'}. \quad (1)$$

There are a number of IP automated measurement routines. Table 1 presents some of the results of the blob analysis on the top image shown in Fig. 6.

## 3.7. Image processing in the frequency domain

Any function can be represented in terms of variables in the frequency or Fourier space. The Fourier transformation of a function $f(x)$ in the Cartesian space in one dimension immediately extended to more dimensions is presented below (Eqs. (2) and (3)). Eq. (4) gives the bidimensional inverse Fourier transformation that allow us to convert a function previously converted to the frequency space back to the Cartesian space. In the mean time, the function can be processed in different ways. For instance, the high frequencies corresponding to noise (Fig. 4) in the image can be removed from $F(kx,ky)$. Fourier filtering is one of the most powerful IP procedures [1,5,6,8].

$$F(k) = \int_{-\infty}^{+\infty} f(x)eikx\,dx, \quad (2)$$

$$F(k,w) = \int\int\int\int_{-\infty}^{+\infty} f(x,y,z,t)e^{i(k.r+wt)}dxdydzdt, \quad (3)$$

Table 1. Characterisation parameters. Results of the blob analysis on the image of Fig. 6.

| Label | Area | Perimeter | Convex Perimeter | Rough-ness | Length | Elonga-tion | Min. Pixel | Max. Pixel | St. Dev. of Pixels | Centroid X (Gray) | Centroid Y (Gray) |
|---|---|---|---|---|---|---|---|---|---|---|---|
| 1 | 14 | 16.24 | 14.97 | 1.085 | 5.638 | 2.271 | 59 | 121 | 17.18 | 723.2 | 18.62 |
| 2 | 16 | 17.66 | 16.62 | 1.062 | 6.281 | 2.466 | 87 | 120 | 8.235 | 698.4 | 23.48 |
| 8 | 18 | 20.49 | 19 | 1.078 | 7.99 | 3.546 | 75 | 118 | 13.99 | 675.1 | 37.71 |
| 9 | 28 | 32.49 | 30.5 | 1.065 | 14.28 | 7.285 | 34 | 114 | 22.54 | 65.87 | 38.25 |
| 17 | 29 | 32.63 | 29.33 | 1.112 | 14.28 | 7.035 | 42 | 121 | 22.05 | 679.9 | 44.84 |
| 29 | 33 | 47.31 | 44.44 | 1.065 | 22.17 | 14.89 | 30 | 120 | 24.14 | 69.58 | 51.59 |
| 35 | 111 | 102.2 | 93.79 | 1.09 | 48.84 | 21.49 | 41 | 121 | 18.39 | 20.59 | 64.62 |
| 36 | 11 | 24.49 | 21.98 | 1.114 | 11.27 | 11.54 | 98 | 122 | 7.192 | 47.5 | 53.98 |
| 37 | 24 | 28.49 | 26.72 | 1.066 | 12.29 | 6.293 | 34 | 119 | 24.22 | 89 | 54.33 |
| 41 | 10 | 18.24 | 16.84 | 1.083 | 7.847 | 6.157 | 86 | 119 | 10.55 | 65.4 | 55.11 |
| 47 | 231 | 96.08 | 81.5 | 1.179 | 42.62 | 7.864 | 30 | 122 | 28.48 | 168.8 | 66.53 |
| 53 | 11 | 13.66 | 12.84 | 1.064 | 4.225 | 1.623 | 66 | 119 | 16.43 | 123 | 59.01 |
| 56 | 10 | 22.83 | 21.58 | 1.058 | 10.46 | 10.94 | 67 | 116 | 15.72 | 71.49 | 59.66 |
| 62 | 16 | 26.49 | 24.01 | 1.103 | 11.9 | 8.847 | 86 | 121 | 11.81 | 659.7 | 6.57 |

$$f(x,y) = \frac{1}{4\pi 2}\int_{-\infty-\infty}^{+\infty+\infty} F(k_x,k_y)e^{-i(kxx+kyy)}dk_x dk_y. \quad (4)$$

The convolution (Eq. (5)) of two functions, *f(x,y)* and *g(x,y)*, is extremely useful in IP; it can be easily implemented in the frequency space with respect to the fact that the Fourier transformation of the convolution of two functions equals to the product of the Fourier transformation of those functions.

$$f(x,y) \otimes g(x,y) = h(x,y) =$$

$$\int_{-\infty}^{+\infty} f(x,y)g(X-x,Y-y)dx,dy. \quad (5)$$

## 4. A CASE STUDY

Ceramic coatings of engineering materials such as Zirconia ($ZrO_2$) partially or totally stabilized by oxides such as $Y_2O_3$, MgO, or $Al_2O_3$ are used for a variety of technological applications requiring thermal insulation, wear and erosion resistance or protection from oxidation, sulfidation and hot corrosion [16]. These kinds of coatings have been applied as Thermal Barrier Coatings (TBCs) for protection of metallic components in gas turbines (vanes, blades, shrouds, *etc*.) and diesel engines, and are also use to improve performance at high temperatures [20].

It allows increase in operating temperature and/or reducing the cooling systems due to the temperature gradient across the thick ceramic coating, that permits better thermodynamic performance, lower emission without requiring major alloy development. TBCs, traditionally, consist of a thick stabilized $ZrO_2$ top coating commonly deposited by atmospheric plasma spraying (APS) on super-alloys precoated with a metallic bond coat (NiCoCrAlY) produced by vacuum plasma spraying (VPS). The $ZrO_2$ top coating has a porous and laminar structure and consists of splats with cracks perpendicular to the surface. This porous structure allows the increase in the thermal isolation and the cracks permit better stresses accommodation [19, 21]. The metallic bond coat improves the diffusion of contaminants and the mismatches of the thermal expansion between the top coat and substrate; this form increases the operation lifetime of the components.

Nowadays higher operation temperatures are required, therefore, in order to obtain systems of coatings that allow these temperature ranges, we need to develop new materials for coatings or new architectures for the existents materials. These new concepts of TBCs should have lower thermal conductivity, and to be stable at higher temperatures [22, 23].

In order to obtain better thermal isolation, in we present here a new concept of TBC. It consists of a conventional bond coat and a graded $ZrO_2$- 8 wt.%$Y_2O_3$ top coat. Below we report a few results of the study of structural properties of $ZrO_2Y_2O_3$ multilayered coatings focusing on the porosity of the

**Table 2.** Coating porosity measured by image analysis and Hg-porosimetry.

| Samples | HP | GPI | GPII | GPIII |
|---|---|---|---|---|
| Hg -Porosity (%) | 14.75 | 15.31 | 15.29 | 13.38 |
| Image Analysis (%)[a] | 11.79 | 13.08 | 15.48 | 13.34 |
| Image Analysis (%)[b] | 11.15 | 10.76 | 12.73 | 9.34 |
| Image Analysis after annealing (%)[a] | 8.44 | 8.33 | 9.90 | 10.57 |
| Image Analysis after annealing (%)[b] | 6.94 | 7.99 | 7.40 | 8.27 |

[a]Porosity with small cracks and ribbons.
[b]Porosity without ribbons.

microlayers. In order to increase the efficiency of the thermal barrier, the different layers should have different porosity increasing towards the surface.

The SEM images were processed using dedicated routines in order to measure the porosity of the coatings [6, 24, 25]. Not only the porosity values for each layer were obtained, but also the way the porosity changes along the coatings cross-section was evaluated. For comparison, the porosity was also determined by the conventional mercury intrusion method [25]. The SEM images were processed to analyze the microstructure (Fig. 6) and to determine the thickness of each microlayer for the different porosities along cross section (Table 2) of all coatings. After annealing in air, all coatings present a sintering structure and a reduction in porosity contents [21]; a thermal grow oxide (TGO) is also observed between the bond and the top coat.

The porosity in thermal barrier coatings is traditionally characterized qualitatively by microstructure observation and quantitatively by mercury intrusion porosimetry (MIP) technique, in addition, coating density measurement are used. The direct examination of coatings microstructure from the cross-sections of a coating using a scanning electron microscopy (SEM) gives comparative information about the porosity of the different coatings. The chemical composition of the microstructure is represented in the images by grey level variation. Pores appear as a very dark areas allowing us to distinguish and quantify them by image analysis. Note that by this method we can not obtain information about the 3-D pore network or connectivity between them [24, 25]. Two series of SEM images were acquired for our analysis, one with 400X magnification and other with 500X magnification.

Using the MIP, it is possible to perform measurements of total porosity for the open pores and to evaluate the pore size distribution. MIP provides information about the connectivity of the pores and microscopy reveals information about a pore geometry, so it looks reasonable to combine these two techniques for a more complete analysis.

The digital micrographs were evaluated by Matrox II program for image analysis. The pores were identified by thresholding of the pores brightness to produce a binary image. The dark area fraction in the binary image was evaluated and the pores percentage was determined [6]. The corresponding porosity values for the different coatings are presented in Table 2.

Analyzing Table 2, one can see a considerable difference between the measured Hg-porosity and the porosity evaluated by image analysis 2. A reduction in the porosity values after annealing has been also determined for all samples, we attribute

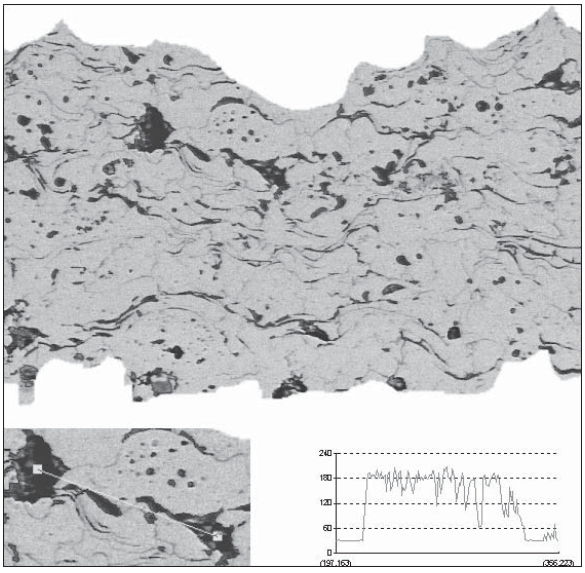

**Fig. 6.** SEM micrograph of a $ZrO_2$ - 8wt.%$Y_2O_3$ coating produced by APS. The image was processed for blob analysis and one profile of a relevant zone of the image is presented (bottom).

it as being mainly due to the sintering effects [26,27]. Hg-porosimeter gives reasonable results for the measurements of small pores and microcracks, but it fails for pores with radii larger than 60 mm. On the other hand, the image analysis gives acceptable results of the porosity due to the contribution of small pores and small microcracks between lamellae within the plasma-sprayed coatings, in addition, the big pores are measured easily. We estimate the thickness of each microlayer in the graded coatings using the SEM analysis data and deposition parameters and the porosity values of each layer were determined by image analysis. The porosity increase from the interface with bond coat to the surface; some decrease in porosity values is noticed for higher values of power deposition. An increase in the working distance also leads to an increase in porosity. For the sample with the constant deposition parameters, we observe a little decrease in the porosity values to the surface that is justified by increase in the substrate temperature during deposition.

## 5. CONCLUSIONS AND FUTURE TRENDS

A major increase in the power and sophistication of modem computing with the implementation of optical computing and distributed and parallel processing will boost the application of image digitalization and processing including in real-time situations. An extended concept of image above the traditional optical definition is already accepted in this field. The processing of bi (or even multi) dimensional functions will allows us humans to perform easier and more effective inspection and evaluation tasks. The gap between the efficiency of our visual systems and those of future imaging and image processing machines will be steadily closed given us even more valuable efficient non invasive automated inspection and diagnostic tools in nanosciences and technologies.

## ACKNOWLEDGMENTS

We would like to acknowledge Prof. V. Teixeira and Dr. A. Portinha for their invaluable collaboration in part of the work herein presented.

## REFERENCES

[1] J.C. Russ, *The Image Processing Handbook. Second ed*. (Boca Raton, Florida: CRC Press, 1995).

[2] D.E. Dudgeon and R.M. Mersereau, *Multidimensional Digital Signal Processing* (Englewood Cliffs, New Jersey: Prentice-Hall, 1984).

[3] K.R. Castleman, *Digital Image Processing. Second ed. 1996* (Englewood Cliffs, New Jersey: Prentice-Hall, year).

[4] C.R. Giardina and E.R. Dougherty, *Morphological Methods in Image and Signal Processing* (Englewood Cliffs, New Jersey: Prentice-Hall, 1988).

[5] R.C. Gonzalez and R.E. Woods, *Digital Image Processing* (Reading, Massachusetts: Addison-Wesley, 1992).

[6] Manuel F.M. Costa // *The Imaging Science Journal* **48** (2001) 177.

[7] Manuel F.M. Costa and Sandra Franco, In: *Improving contact lens' fitting evaluation by the application of image processing techniques* (International Contact Lens Clinic, Butterworld 25,1, January/February, 1988) p. 22.

[8] J.W. Goodman, *Introduction to Fourier Optics* (McGraw-Hill Physical and Quantum Electronics Series., New York: McGraw-Hill, 1968) 287.

[9] H.J.A.M. Heijmans, *Morphological Image Operators. Advances in Electronics and Electron Physics* (Boston: Academic Press, 1994).

[10] I.T. Young // *IEEE Engineering in Medicine and Biology* **15** 1996. 59.

[11] I.T. Young and L.J. Van Vliet // *Signal Processing* **44** (1995) 139.

[12] L.J. Van Vliet, I.T. Young and A.L.D. Deckers // *Computer Vision, Graphics, and Image Processing* **45** (1989) 167.

[13] F. Meyer and S. Beucher // *J. Visual Comm. Image Rep.* **1** (1990) p. 21.

[14] Manuel F.M. Costa, In: Proceedings of the International Conference on Composite Engineering, ed. by. D. Hui (ICCE/7, Denver, CO, USA, July 2000) p. 57.

[15] M. F. Cerqueira, J. A. Ferreira, M. Andritschky and Manuel F. M. Costa // *Microelectronic Engineering* **43-44** (1998) 627.

[16] Z. Ji, J.A. Haynes, M.K. Ferber and J.M. Rigsbee // *Surf. Coat. Tech.* **135** (2001) 109.

[17] R. Guinebretiere, B. Soulestin and A. Douger // *Thin Solid Films* **319** (1998) 197.

[18] C.R. Aita, M.D. Wiggins, R. Whig and C.M. Scanlan //*J. Appl. Phys.* **79** (1996) 1176.

[19] J.S. Kih, H.A. Marzouk and P.J. Reucroft // *Thin Solid Films* **254** (1995) 33.
[20] Jeanine T. DeMasi-Marcin and Dinesh K. Gupta // *Surf. Coat. Tech.* **68/69** (1994) 1.
[21] Lech Pawlowski, Didier Lombard and Pierre Fauchais // *J. Vac. Sci. TechnoL,* **A3** (1985) 2494.
[22] R. Vaßen and D. Stöver, *Conventional and new materials for thermal barrier coatings. Functional Gradient Materals and Surface Layers Prepared by fine Particles Technology* (Kluwer Academic Publishers, Netherlands, 2001).
[23] D. Stöver and C. Funke // *J. of Materials Processing Technology* (1999) **92-93** 195.
[24] K. Mailhot, F. Gitzhofer and M.I. Boulos, In: *Proceedings of the 15th International Thermal Spray Conference,* (Nice, France, 25-29 May, 1998) p. 917.
[25] A.B. Abell, K.L. Willis, and D.A. Lange // *Journal of Colloid and Interface Science* **211**(1999) 39.
[26] B. Siebert, C. Funke, R. Vaßen and D. Stöver // *J. of Materials Processing Technology* **92-93** (1999) 217.
[27] R. Vaßen, N. Czech, W. Mallener, W. Stamm and D. Stöver // *Surf. Coat. Tech.* **141** (2001) 135.